JOURNAL OF AIRCRAFT
Vol. 35, No. 2, March–April 1998

Simulations of Wind Along Flight Trajectories in the Ocean Surface Layer

Bård Venås* and Lars R. Sætran†
Norwegian University of Science and Technology, N-7034 Trondheim, Norway

A simulation model for numerical realizations of turbulence along flight trajectories in the atmospheric ocean surface layer is developed and tested. The model is based on a Monte Carlo simulation technique in which a digitally generated random signal is filtered to represent a random realization of the target process. In addition to purely atmospheric/shear-driven turbulence, the model includes a surface perturbation effect on the wind field caused by the underlying wave surface. It is shown that the wind fluctuations may take varying forms, depending on factors such as flight direction, flight height, and wave state. The differences found in frequency contents may be of crucial importance for the design of control systems for flight vehicles operating in this type of climate, such as sea-skimming missiles.

Nomenclature

C	=	wave velocity, m/s
$F\{\ \}$	=	Fourier transform
H_s	=	significant wave height, m
$\mathcal{H}_{fg}(\boldsymbol{k})$	=	filter function in Fourier space, $F\{h_{fg}(\boldsymbol{x})\}$
$h_{fg}(\boldsymbol{x})$	=	filter function between processes f and g
$h(x, y)$	=	wave elevation, m
$\boldsymbol{k}$	=	wave number vector, (k_x, k_y, k_z), rad/m
L_u, L_v, L_w	=	turbulence length scales for u, v, and w fluctuations, respectively, m
R_{fg}	=	correlation between processes f and g
S_{fg}	=	cross spectrum, $F\{R_{fg}\}$
$\mathcal{U}', \mathcal{V}', \mathcal{W}'$	=	Fourier transform of $\boldsymbol{u}'$, $F\{\boldsymbol{u}'\}$
$\mathcal{U}_w, \mathcal{V}_w, \mathcal{W}_w$	=	Fourier transform of $\boldsymbol{u}_w$, $F\{\boldsymbol{u}_w\}$
$U(z)$	=	mean velocity, m/s
U_{10}	=	reference velocity, $U(z = 10$ m), m/s
$\hat{\boldsymbol{u}}$	=	wind velocities in trajectory following coordinates $(\hat{x}, \hat{y}, z)$, $(\hat{u}, \hat{v}, w)$, m/s
$\boldsymbol{u}_w(\boldsymbol{x})$	=	wave-induced wind fluctuations, m/s
$\boldsymbol{u}(\boldsymbol{x}, t)$	=	wind velocity vector in Cartesian coordinates
$\boldsymbol{u}'(\boldsymbol{x}, t)$	=	wind fluctuations, m/s
$\mathcal{W}_n$	=	white noise in Fourier space
w_n	=	white noise
$\boldsymbol{x}$	=	Cartesian coordinates, (x, y, z): x in the streamwise direction, m; y in the transverse direction, m; and z in the vertical direction, m
$\hat{\boldsymbol{x}}$	=	trajectory following coordinates $(\hat{x}, \hat{y}, z)$: $\hat{x}$ in the flight direction, m; $\hat{y}$ transverse to the flight direction, m; and z in the vertical direction, m
α	=	flight direction in the (x, y) plane
σ_f	=	standard deviation of process f, $\sqrt{\overline{ff}}$
ω	=	circular frequency, rad/s

Introduction

ATMOSPHERIC flight is by default relative to a turbulent surrounding, and this will always affect flight. Somewhat simplistically one may say that the extent of the influence scales on the ratio between the characteristics of the wind and those of the flight vehicle involved, e.g., velocity, mass, lift curve slope, and maneuvering capability. In the case of a sea-skimming missile at transonic velocities, the flight velocity will be high—at least an order of magnitude—compared with the wind fluctuations even in extreme weather conditions. This implies a higher momentum-to-gust loading ratio than, for instance, for an aircraft at low takeoff or approach speeds. However, to accomplish mission objectives, one will often seek to keep the lowest possible flight altitude for sustained periods of time, making the margins within which the missile operates very small. It is therefore crucial to be able to make realistic estimates about the turbulence and its effect as early as possible in the design phase of a new missile to develop a well-proportioned prototype (in control systems, control surfaces, etc.) and to keep total development costs down.

In the literature, climatic data are available for long-time and short-time wind and wave statistics.[1–3] Long-time statistics describe the expectancy of mean wind velocity, wave states, etc., as functions of climatic zones and are evidently very useful for the definition of system requirements. Short-time statistics, on the other hand, seem more sparse and limited, though factors such as wind spectra and gust factors are relatively well documented.[4–6] These are, however, often difficult to use quantitatively, as most spectral analysis methods require some linear assumption, and gust factors merely are means of extremes and tell little about the specific wind events one may encounter.

The best solution, therefore, often turns out to be analysis through total or partial system simulations in the time–space domain. To provide good results, these simulations need realistic input data of wind components along different flight paths. Such data can be estimated through flight tests, but depending solely on this will in most cases be a rigid and unsatisfactory solution. Numerical realizations of turbulence through the Monte Carlo type of simulation, however, can provide a very flexible and cost-efficient method for generating wind data. Different types of such turbulence realization schemes have been suggested and employed over the years, but the basic idea remains the same: filtering a random input so that the output becomes a random realization of the target process, i.e., satisfying its spectrum.[7,8] Simulations can be performed either on-line, with wind data being calculated along the flight path, or off-line, as flight through a precalculated velocity field. Depending somewhat on the type of simulation chosen, such as the number of physical dimensions or resolution, this technique makes it possible to acquire just the amount of wind data needed.

Presented as Paper 97-0423 at the AIAA 35th Aerospace Sciences Meeting, Reno, NV, Jan. 6–9, 1997; received April 7, 1997; revision received Sept. 16, 1997; accepted for publication Sept. 18, 1997.

*Ph.D. Student, Department of Mechanics, Thermo and Fluid Dynamics.

†Associate Professor, Department of Mechanics, Thermo and Fluid Dynamics. Member AIAA.

This paper discusses a new turbulence simulation model that takes into account special factors, such as the direct influence of waves and anisotropy in the turbulence, that are encountered when flying in the atmospheric ocean surface layer, which is the layer typically ranging from the ocean surface up to z = 50 m.[9]

Wind Climatic Model

Wind effects relevant to missile flight at low altitudes are the purely atmospheric/shear-driven turbulence but may also include mechanical turbulence and changes in the mean wind induced by local terrain along the flight path. For sea-skimming missiles above open waters, the terrain is special in the sense that the main features, the waves, are relatively small, periodic, and in motion. If one conceptually pictures the wavy surface inducing similarly shaped streamlines in the flow close to the surface, this would result in wind fluctuations at the wave frequency, as shown schematically in Fig. 1.

Lesieutre et al.[10] did a preliminary investigation of missiles flying low over waves based on such an assumption, modeling the fluctuations as a harmonic oscillation and showing that wind forcing at typical wave frequencies may lead to control problems, depending, for instance, on the wave state. The wind field they used as input to their aerodynamics and control system simulation is, however, somewhat too simplistic to give fully representative results. First of all, atmospheric turbulence is a stochastic process, having frequency spectra with different characteristics than that of a harmonic wave. Second, the sea surface is far from being a monotonic two-dimensional wave train, and flight paths may take any other direction than that of the wind or wave propagation.

At the same time, numerous offshore measurements have found interaction between the waves and turbulence in the surface layer in the form of additional peaks in the turbulence spectra at the wave frequency.[11,12] This seems to be in accordance with the qualitative model suggested in Fig. 1, if one adds background atmospheric turbulence to a realistic (three-dimensional, not fully periodic) wave-surface wind field perturbation. This is shown in Fig. 2, i.e., the total spectrum seen as the sum of a turbulence spectrum and a wave influence around the wave numbers k of the surface oscillations. In Fig. 2a, both axes are logarithmic, as is custom, and the wave perturbation shows up as a single relatively small peak. However, plotting the figure in linear scaling (Fig. 2b) shows how the energy contained in such a wave influence is much higher than the energy of the turbulence in the same spectral region.

The simulations in this paper are based on a model that takes wave-influence effects into account.[13] The analysis starts by dividing the instantaneous wind velocity vector $\boldsymbol{u}$ into three parts: 1) mean velocity $\boldsymbol{U}$, 2) atmospheric turbulence $\boldsymbol{u}'$ as in standard Reynolds decomposition, and 3) so-called wave-induced fluctuations $\boldsymbol{u}_w$

$$\boldsymbol{u} = \boldsymbol{U} + \boldsymbol{u} + \boldsymbol{u}_w = U + (u', v', w') + (u_w, v_w, w_w) \quad (1)$$

where the rules of Reynolds decomposition apply for both types of fluctuations ($\overline{u'} = \overline{v'} = \overline{w'} = \overline{u_w} = \overline{v_w} = \overline{w_w} = 0$).

The atmospheric turbulence is defined as the part of the total fluctuations that is not correlated to the wave elevation $h(x, y)$. [Generally, a wave surface is also a function of time t, $h = h(x, y, t)$, as are the velocity fluctuations $\boldsymbol{u}'$ and $\boldsymbol{u}_w$, but as will be shown later, we will only consider an instantaneous wind–wave situation and will therefore not take t into consideration.]

$$R_{u'h}(\Delta x, \Delta y, z) = \overline{\boldsymbol{u}'(\boldsymbol{x})h(x + \Delta x, y + \Delta y)} \equiv \boldsymbol{0} \quad (2)$$

whereas $\boldsymbol{u}_w$ is the correlated part and thus a deterministic function of the wave surface

$$R_{u_w h}(\Delta x, \Delta y, z) = \overline{\boldsymbol{u}_w(\boldsymbol{x})h(x + \Delta x, y + \Delta y)} = \boldsymbol{f}(\Delta x, \Delta y, z) \quad (3)$$

where the overbar represents the mean in the (x, y) plane. These definitions further imply that

$$R_{u'u_w}(\Delta \boldsymbol{x}) = \overline{\boldsymbol{u}'(\boldsymbol{x})\boldsymbol{u}_w(\boldsymbol{x} + \Delta \boldsymbol{x})} = \boldsymbol{0} \quad (4)$$

which is to say that there is no correlation between the atmospheric turbulence and the wave-induced fluctuations. The total two-point correlation then takes the following form (leaving the coordinates out for simplicity):

$$\begin{aligned} R_{uu} &= \overline{(\boldsymbol{u} - U)(\boldsymbol{u} - U)} = \overline{(\boldsymbol{u}' + \boldsymbol{u}_w)(\boldsymbol{u}' + \boldsymbol{u}_w)} \\ &= \overline{\boldsymbol{u}'\boldsymbol{u}' + \boldsymbol{u}'\boldsymbol{u}_w + \boldsymbol{u}_w\boldsymbol{u}' + \boldsymbol{u}_w\boldsymbol{u}_w} \\ &= R_{u'u'} + R_{u'u_w} + R_{u_w u'} + R_{u_w u_w} \\ &= R_{u'u'} + R_{u_w u_w} \end{aligned} \quad (5)$$

The Fourier transform of R_{ij} yields the turbulence spectral tensor S_{ij}

$$S_{ij}(\boldsymbol{k}) = F\{R_{ij}\} = \int_{-\infty}^{\infty} R_{ij}(\boldsymbol{x})\exp[-i\boldsymbol{k}\cdot\boldsymbol{x}]\, \mathrm{d}\boldsymbol{x} \quad (6)$$

and because $F\{\ \}$ is a linear operator ($F\{\zeta + \eta\} = F\{\zeta\} + F\{\eta\}$), we find that the total spectrum can be modeled as the sum of a turbulence spectrum and a wave-influence spectrum

$$S_{uu} = S_{u'u'} + S_{u_w u_w} \quad (7)$$

This is qualitatively in good accordance with what is found in the literature[11,12] and was described in the preceding text (Fig. 2), i.e., that spectra above waves contain an extra peak at the wave frequency. If one removes the wave peak from these spectra, the remaining part seems to resemble a standard turbulence spectrum, characterized by a cutoff frequency defined by the length scale and a constant rolloff of the form $k^{-\text{const}}$ for higher wave numbers.

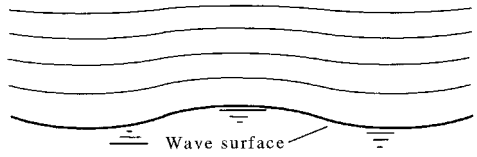

Fig. 1 Conceptual model: streamlines above wave surface.

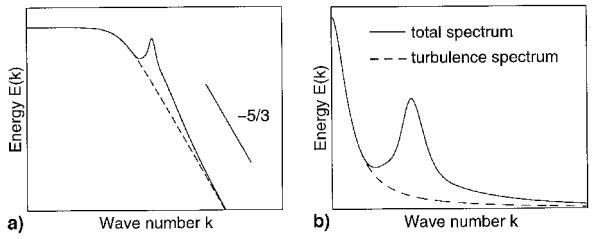

Fig. 2 Total wind spectrum as sum of atmospheric and wave-induced fluctuations: a) logarithmic and b) linear axes.

Model Spectra

In our simulations we have used a standard von Kármán formulation[8,14] to describe the atmospheric turbulence spectral tensor

$$S_{ij}(\boldsymbol{k}) = \frac{110\pi}{9}\sigma^2 a^4 \frac{(|\boldsymbol{k}|^2\delta_{ij} - k_i k_j)}{[1 + (aL|\boldsymbol{k}|)^2]^{17/6}}$$
$$a = 1.339, \qquad i = x, y, z, \qquad j = x, y, z \quad (8)$$

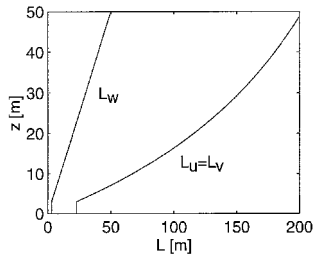

Fig. 3 L_u, L_v, and L_w according to MIL-F-8785C.

The formulation is based on the theory of isotropic turbulence, where the standard deviations σ of fluctuations and length scales L are constant in space and in all directions, i.e., invariant to translation and rotation.

This is generally not the case for turbulence in the atmospheric surface layer. Here, the turbulent stresses can be approximated as being constant with height, but differ between components. The length scales, on the other hand, are both different in components and vary strongly with height. To account for this we used an approach similar to that of Robinson,[8] who used the von Kármán spectra while varying the length scales and turbulence levels with height and component.

Measurements of these scaling quantities vary to a certain extent. We have chosen to use length scales according to American military standard MIL-F-8785C, shown in Fig. 3.[15] The length scale of the vertical fluctuations is approximately proportional to z, whereas the horizontal fluctuations are of substantially larger scale.

In the case of the turbulence levels, one usually finds an approximate 4:3:2 relation between the x, y, and z components in the surface layer (the logarithmic region; see, e.g., Hinze[16]) in wind-tunnel boundary layers. In a survey of full-scale measurements, Tielemann[17] reports the same typically to be the situation for $U < 10$ m/s, whereas it tends toward a 2:2:1 ratio for higher velocities. In our model we have chosen the 4:3:2 ratio, though there is nothing to substantiate that this is the better choice. The overall turbulence level in the mean flow direction is set to 10% of the mean velocity, at $z = 10$ m (U_{10}), and constant with height, typical of the results of, e.g., Tielemann.

The wave-induced fluctuations are modeled[13] with basis in the cross spectra between the fluctuations and the surface elevation, being of the form

$$S_{u_w h}(k_x, k_y, z) = \frac{\sigma_{u_w}(z)}{\sigma_h} S_{hh}(k_x, k_y) \tag{9}$$

$$S_{v_w h}(k_x, k_y, z) = \frac{\sigma_{v_w}(z)}{\sigma_h} \exp\{-(\pi/2)[\mathrm{sgn}(k_x) - \mathrm{sgn}(k_y)]i\} \times S_{hh}(k_x, k_y) \tag{10}$$

$$S_{w_w h}(k_x, k_y, z) = \frac{\sigma_{w_w}(z)}{\sigma_h} \exp[-(\pi/2)\mathrm{sgn}(k_x)i] S_{hh}(k_x, k_y) \tag{11}$$

where $S_{hh}(k_x, k_y)$ is the wave elevation spectrum.

There are several so-called model spectra for wave elevation, mainly based on data from offshore measuring stations. In our simulations we used one of these, the Joint North Sea Wave Project (JONSWAP) spectrum $S_{hh}(\omega)$, which is recommended for partially developed waves as found in coastal and landlocked areas.[1] We have in addition used the directional spectrum (propagation as function of direction) of Hasselmann et al.[18] to transform this frequency spectrum into a two-dimensional spatial spectrum $S_{hh}(k_x, k_y)$, which is used as input to the model.

The wave-induced fluctuations decay with height according to the standard deviations in Eqs. (9–11). We have based these σ ratios on the measurements of Venås et al.,[13] where linear curve fits give

$$\frac{\sigma_{u_w}(z)}{\sigma_h} = \frac{0.055(1 - 0.13z/H_s)U_{10}}{H_s/4} \tag{12}$$

$$\sigma_{v_w}(z) = \frac{\sigma_{u_w}(z)}{2} \tag{13}$$

$$\sigma_{w_w}(z) = \sigma_{u_w}(z) \tag{14}$$

for $z/H_s < 7.5$, i.e., a 2:1:2 ratio between the components. Note that these measurements were performed using a rigid wave surface, thus representing zero wave velocity C. This is naturally not realistic but, as the wave velocity and direction may be any other than those of the wind, this represents one extreme of the situation $U > C$. It may be useful to compare similar experiments for other values of U/C to these results.

Simulation Model

As stated in the Introduction, Monte Carlo simulations are based upon sending random signals through suitable filters. In Fourier space this takes the form of a multiplication of the Fourier transforms of $h_{fg}(\boldsymbol{x})$ and a random input $g(\boldsymbol{x})$

$$\mathcal{F}(\boldsymbol{k}) = \mathcal{H}_{fg}(\boldsymbol{k})\mathcal{G}(\boldsymbol{k}) \tag{15}$$

If $F^{-1}\{\ \}$ is the inverse Fourier transform, a realization of the process f is now obtained as

$$f = F^{-1}\{\mathcal{F}\} \tag{16}$$

In our simulations we use white noise w_n as input, i.e., a signal that is totally uncorrelated to itself. The power spectrum of this signal is uniform in the mean, signifying that the energy is equally distributed at all frequencies

$$S_{w_n w_n}(\boldsymbol{k}) = F\{R_{w_n w_n}(\boldsymbol{x})\} = \sigma_{w_n}^2 \tag{17}$$

where $\sigma_{w_n}^2$ is the variance of the signal. $\mathcal{H}_{fg}$ is found from one of the two formulas[19]

$$S_{ff} = |\mathcal{H}_{fg}|^2 S_{gg} \Rightarrow \mathcal{H}_{fg} = \sqrt{S_{ff}/S_{gg}} \tag{18}$$

$$S_{fg} = \mathcal{H}_{fg} S_{gg} \Rightarrow \mathcal{H}_{fg} = S_{fg}/S_{gg} \tag{19}$$

where Eq. (18) represents only the gain factor, whereas Eq. (19) also includes the phase difference between the two signals. If S_{ff} is the power spectrum of the desired output, and the input is white noise, we get the filters

$$\mathcal{H}_{fg} = \sqrt{S_{ff}/S_{gg}} = (1/\sigma_{w_n})\sqrt{S_{ff}} \tag{20}$$

$$\mathcal{H}_{fg} = S_{fg}/S_{gg} = (1/\sigma_{w_n})S_{fw_n} \tag{21}$$

Generally, when simulating a turbulent velocity field, one may be interested in the three-dimensional velocity vector in three-dimensional space, possibly as a function of time. However, the fact that the missile travels at a speed at least one order of magnitude higher than that of the wind allows one to approximate the instantaneous velocity field as frozen (in the sense of Taylor's hypothesis for turbulent flows), so that we can simulate solely in space.

The different wind fluctuations are generally correlated to each other, and this can be accounted for by using a number of independent white noise inputs $\mathcal{W}_{n1,2,3}$ and filters $\mathcal{H}_{ij}$, for instance, on the form

$$\begin{bmatrix} \mathcal{H}_{11} & 0 & 0 \\ \mathcal{H}_{21} & \mathcal{H}_{22} & 0 \\ \mathcal{H}_{31} & \mathcal{H}_{32} & \mathcal{H}_{33} \end{bmatrix} \begin{bmatrix} \mathcal{W}_{n1} \\ \mathcal{W}_{n2} \\ \mathcal{W}_{n3} \end{bmatrix} = \begin{bmatrix} \mathcal{U}' \\ \mathcal{V}' \\ \mathcal{W}' \end{bmatrix} \tag{22}$$

$\mathcal{H}_{ij}$ can be designed from the power spectra S_{ij} as shown in Robinson.[8] Based on the model formulated in Eqs. (9–11), one could then have defined filter functions of this type and simulated the full velocity field in three dimensions.

There are, however, some problems to this. First, to include all correlations, the simulation domain has to be three-dimensional, which is computationally demanding and produces a large amount of redundant data because the missile traverses the domain along a single trajectory. Second, such a simulation is difficult and time-consuming because the length scales, and thus the spectra, vary significantly with altitude through the surface layer, and this has to be accounted for. Based on this, it was chosen to simulate the three different atmospheric turbulence components independently to create a more flexible model

$$\begin{bmatrix} \mathcal{H}_{uw_n} & 0 & 0 \\ 0 & \mathcal{H}_{vw_n} & 0 \\ 0 & 0 & \mathcal{H}_{ww_n} \end{bmatrix} \begin{bmatrix} \mathcal{W}_{n1} \\ \mathcal{W}_{n2} \\ \mathcal{W}_{n3} \end{bmatrix} = \begin{bmatrix} \mathcal{U}' \\ \mathcal{V}' \\ \mathcal{W}' \end{bmatrix} \tag{23}$$

This is not strictly physically correct, as we lose the intercorrelation between the different turbulence components. However, because the vertical component was considered the single most important issue (it directly alters the angle of attack in the most critical direction), Eq. (23) was considered a fair approximation.

This approach further allows one to perform simulations along flight trajectories by defining a trajectory-following coordinate system $(\hat{x}, \hat{y}, z)$, where the top symbols signify that the axes have been rotated an angle α to follow the flight path, while z is kept vertical (Fig. 4). It follows that the turbulence is isotropic in the (x, y) plane (L_u and L_v are equal), and that S_{ij} thus is invariant to rotation in this plane. The anisotropy included in the turbulence levels, however, follows the wind coordinates and has to be rotated according to α.

The wave-induced fluctuations are all deterministic functions of $h(x, y)$ and are therefore fully correlated to each other. Filter functions including the intercorrelations can be found by combining Eqs. (19) and (20), so that

$$\mathcal{H}_{uw_n} = \mathcal{H}_{uh}\mathcal{H}_{hw_n} = \frac{S_{u_w h}(k_x, k_y, z)}{S_{hh}(k_x, k_y)}\mathcal{H}_{hw_n} = \frac{\sigma_{u_w}(z)}{\sigma_h \sigma_{w_n}}\sqrt{S_{hh}} \tag{24}$$

$$\mathcal{H}_{vw_n} = \mathcal{H}_{wh}\mathcal{H}_{hw_n} = \frac{S_{v_w h}(k_x, k_y, z)}{S_{hh}(k_x, k_y)}\mathcal{H}_{hw_n} = \frac{\sigma_{v_w}(z)}{\sigma_h \sigma_{w_n}}\exp\{-(\pi/2)[\mathrm{sgn}(k_x) - \mathrm{sgn}(k_y)]i\}\sqrt{S_{hh}} \tag{25}$$

$$\mathcal{H}_{ww_n} = \mathcal{H}_{wh}\mathcal{H}_{hw_n} = \frac{S_{w_w h}(k_x, k_y, z)}{S_{hh}(k_x, k_y)}\mathcal{H}_{hw_n} = \frac{\sigma_{w_w}(z)}{\sigma_h \sigma_{w_n}}\exp[-(\pi/2)\mathrm{sgn}(k_x)i]\sqrt{S_{hh}} \tag{26}$$

where $\mathcal{H}_{hw_n} = \mathcal{H}_{hw_n}(k_x, k_y)$ is the transfer function between the wave surface and white noise. The intercorrelations are automatically accounted for in the model by simulating the fluctuations in the two-dimensional (k_x, k_y) plane, scaling for height using Eqs. (12–14) and applying the same white noise source for all three fluctuations.

The total simulation model is thus of the form

$$\begin{bmatrix} \mathcal{H}_{uw_n} & 0 & 0 \\ 0 & \mathcal{H}_{vw_n} & 0 \\ 0 & 0 & \mathcal{H}_{ww_n} \end{bmatrix} \begin{bmatrix} \mathcal{W}_{n1} \\ \mathcal{W}_{n2} \\ \mathcal{W}_{n3} \end{bmatrix} + \begin{bmatrix} \mathcal{H}_{u_w w_n} \\ \mathcal{H}_{v_w w_n} \\ \mathcal{H}_{u_w w_n} \end{bmatrix} [\mathcal{W}_{n4}] = \begin{bmatrix} \mathcal{U}' + \mathcal{U}_w \\ \mathcal{V}' + \mathcal{V}_w \\ \mathcal{W}' + \mathcal{W}_w \end{bmatrix} \tag{27}$$

where the two types of fluctuations are simulated separately.

Phenomenological Simulation

As argued in the preceding text, probably the most important wind component in our case is the vertical one. The turbulence length scales define the cutoff frequency of the spectra and change significantly throughout the surface layer. The characteristic scale for the wave influence, on the other hand, is the wavelength. In high seas, say, $H_s = 5$ m, the wavelength will typically be on the order of 100 m or more,[3] and the spatial scale of the wave-induced fluctuations will thus be substantially larger than those of the vertical turbulence. To get an impression of this, Fig. 5a shows a cut along the (x, z) plane of turbulence fluctuations from a three-dimensional simulation. Figure 5b shows the wave-induced fluctuations in the same plane, and Fig. 5c shows the total fluctuations. Figures 5a–5c are plotted together with the corresponding simulated wave surface.

From Fig. 5 we see that the turbulence spatial structures are very small near the surface and become larger with height. The wave-induced fluctuations can be perceived as a filtering of the wave surface, and we see that there is a positive (upward) perturbation at the windward side of the waves and a negative one at the leeward sides.

The wave surface used here is a JONSWAP realization, with characteristic scales set to a wavelength of 100 m and a significant wave height of 5 m. Even though these values correspond to quite choppy seas, the wave-induced fluctuations are of a much lower frequency than the atmospheric turbulence.

The color scale in Fig. 5 is nondimensionalized with U_{10}, and we see that the total values reach fluctuation levels of

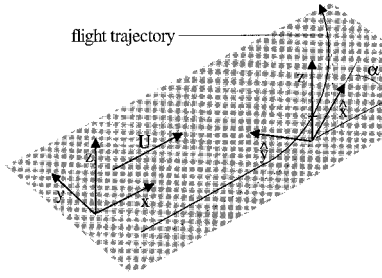

Fig. 4 Definition of trajectory-following coordinate system $(\hat{x}, \hat{y}, z)$.

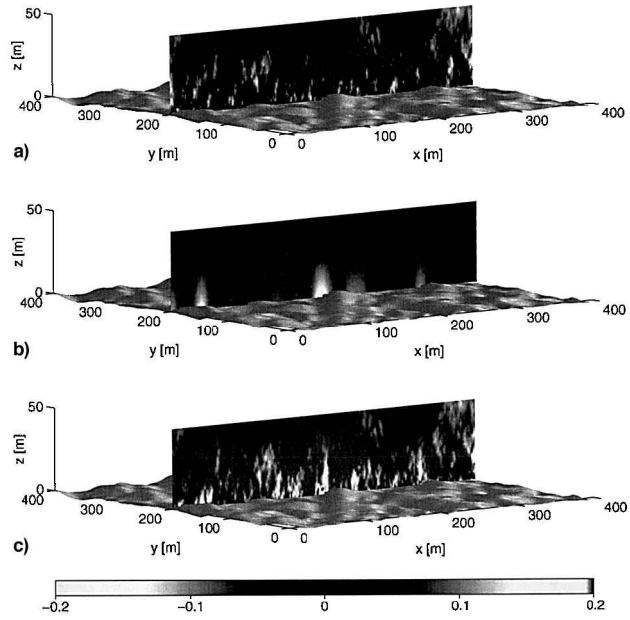

Fig. 5 Phenomenological simulation: vertical wind components in $(\hat{x}, z)$ plane along mean wind direction a) w'/U_{10}, b) w_w/U_{10}, and c) w/U_{10}.

approximately ±20% of U_{10} in this short realization. At typical tough-weather conditions, the wind velocity may be approximately one-tenth of the missile velocity. Such a situation would thus lead to frequent perturbations in missile angle of attack up to more than ±1 deg, a gust level for which Lesieutre et al.[10] found possibilities for mission failure when flying close to the sea surface.

Simulations Along Flight Trajectories

To exemplify the physics described by the model, we simulated some relatively basic flight paths. U_{10} is set to 25 m/s, and the wave state is as it was in the preceding text (length, 100 m, significant height, 5 m).

First, the difference between the turbulent and the wave-induced fluctuations can easily be seen in Fig. 6, which shows the same situation as before: vertical fluctuations in flight along the wind direction. The turbulent fluctuations have a high frequency (length scale 10 m), and the wave-induced fluctuations have a mean length of about 100 m, in other words, 10 fluctuations per 1000 m. The energy content in the two types of fluctuations is, however, relatively equal.

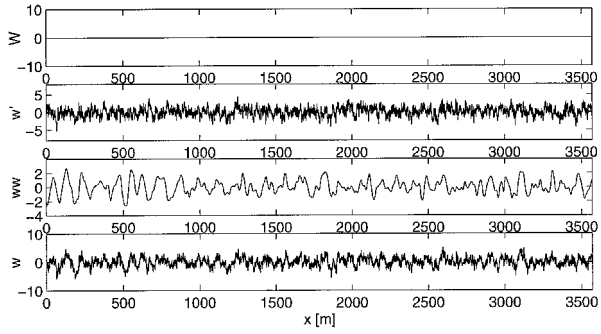

Fig. 6 Simulated vertical velocities w for flight path along the mean wind/wave direction.

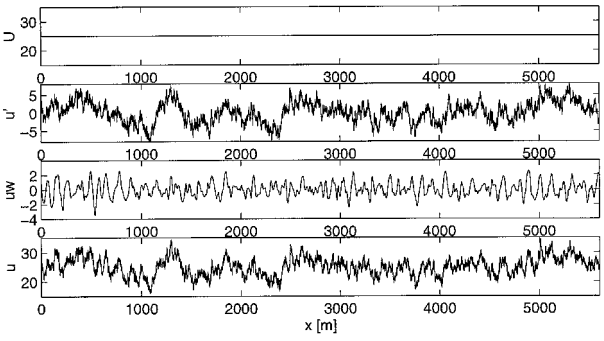

Fig. 7 Simulated $\hat{u}$ for flight path along the mean wind/wave direction.

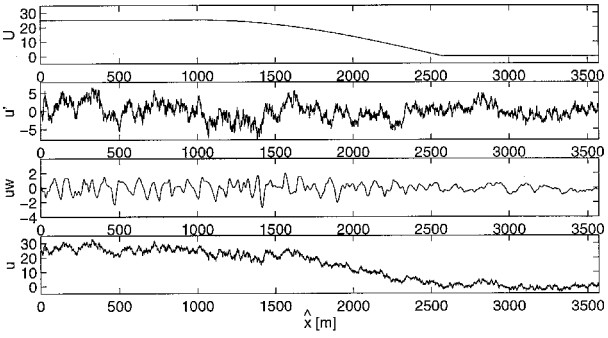

Fig. 8 Simulated $\hat{u}$ for flight path along wind/wave–curve–cross-wind/wave.

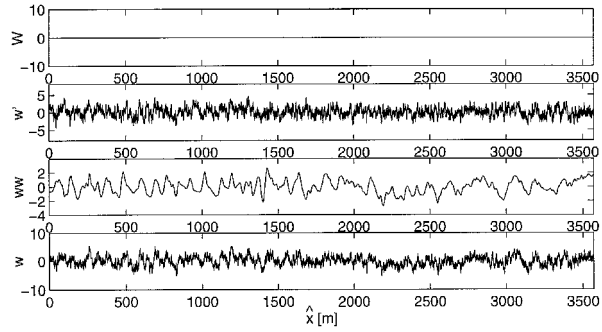

Fig. 9 Simulated w for flight path along wind/wave–curve–cross-wind/wave.

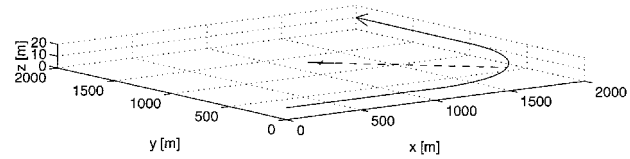

Fig. 10 Flight path for simulations shown in Figs. 8 and 9.

Figure 7 shows the fluctuations in the mean wind/wave direction from the same simulation as Fig. 6. We see a remarkable difference in the character of the two fluctuations: the turbulence is spread over a much wider frequency range than the wave influence, the low-frequency turbulence fluctuations lasting several wavelengths while the smaller ones are much shorter than the waves. Further, even though there is more energy in the turbulence than in the wave perturbations, the total fluctuations seem more peaked than the turbulence. This is because of the extra energy within the relatively narrow frequency band of the waves.

Both types of fluctuations vary strongly depending on flight direction. This point can be seen from Figs. 8 and 9, which show a simulation along a portion of a flight path (see Fig. 10) that starts out along the wind direction ($\hat{x}$ = 0–1000 m), goes through a 1000-m-radius, 90-deg circular curve ($\hat{x}$ = 1000–2570 m), and finally continues 1000 m in the new direction (along the y axis). In the first part of the simulation we can see the same characteristics as in Figs. 6 and 7. However, through the turn, the characteristics gradually change.

First considering the turbulence, the length scales follow the trajectory, and the frequency contents remain constant throughout the curve. The turbulence levels, however, follow the wind coordinates: we see that the fluctuations along the path are reduced somewhat, whereas the vertical fluctuations are not altered.

The greatest differences are found in the wave influence. We see that the frequency contents change in all components. This is because the flight direction gradually changes from along the wind to along the wave tops, and the wave width is not periodic, as are the wavelengths.[13] This is to say, all wave fluctuations are quite periodic in flight along the wind but lose periodicity when at an angle to the wind. The fluctuation levels, on the other hand, follow the wind/wave propagation direction, and the stronger horizontal fluctuation ($\hat{u}_w = u_w$) turns in to the perpendicular one with respect to the flight path after the curve ($\hat{v}_w = u_w$).

Conclusions

This paper provides a model for relatively detailed simulations of turbulence in the atmospheric ocean surface layer, including wave perturbation of the wind field as caused by the underlying wave surface. It is shown that the wind fluctuations may take varying forms, depending upon factors such as flight

direction, flight height, and wave state. Possibly the most important result of the test simulations reported here is the substantial difference in frequency contents between purely atmospheric turbulence and wave-induced fluctuations. This may be of crucial importance for the design of control systems for flight vehicles operating in this type of climate, such as sea-skimming missiles.

Acknowledgment

This work was sponsored by Kongsberg Aerospace through the New Anti-Ship Missile Program.

References

[1]Bales, S. L., Lee, W. T., and Voelker, J. M., "Standardized Wave and Wind Environment for NATO Operational Areas," David Taylor Research Center, DTNSRDC/SPD-0919-01, Bethesda, MD, 1981.

[2]Avara, E. P., and Miers, B. T., "Surface Wind Speed Distributions," ASL-TR-0313, White Sands Missile Range, NM, 1992.

[3]*Global Wave Statistics*, compiled and edited by British Maritime Technology Ltd., Unwin Brothers, Surrey, England, UK, 1991.

[4]Jensen, N. O., and Busch, N. E., "Atmospheric Turbulence," *Engineering Meteorology*, edited by E. Plate, Elsevier, Amsterdam, 1982, pp. 179–231.

[5]Smith, S. D., and Chandler, P. C. P., "Spectra and Gust Factors for Gale Force Marine Winds," *Boundary-Layer Meteorology*, Vol. 40, No. 4, 1987, pp. 393–406.

[6]Brown, R. D., and Swail, V. R., "Over-Water Gust Factors," *Ocean Engineering*, Vol. 18, No. 4, 1991, pp. 363–394.

[7]Beal, T. R., "Digital Simulation of Atmospheric Turbulence for Dryden and von Karman Models," *Journal of Guidance, Control, and Dynamics*, Vol. 16, No. 1, 1993, pp. 132–138.

[8]Robinson, P. A., "The Modeling of Turbulence and Downburst for Flight Simulators," Ph.D. Dissertation, Univ. of Toronto, Toronto, ON, Canada, 1991.

[9]Arya, S. P., "Atmospheric Boundary Layers over Homogeneous Terrain," *Engineering Meteorology*, edited by E. Plate, Elsevier, Amsterdam, 1982, pp. 233–267.

[10]Lesieutre, D. J., Nixon, D., Dillenius, M. F. E., and Torres, T. O., "Analysis of Missiles Flying Low over Various Sea States," *AIAA Atmospheric Flight Mechanics Conference* (Portland, OR), AIAA, Washington, DC, 1990, pp. 425–434.

[11]Antonia, R. A., and Chambers, A. J., "Wind-Wave-Induced Disturbances in the Marine Surface Layer," *Journal of Physical Oceanography*, Vol. 10, April 1980, pp. 611–622.

[12]Miller, S. D., Friehe, C. A., Hristov, T. S., and Edson, J. B., "Profiles of Wind Speed and Reynolds' Stress over the Ocean," Third International Symposium on Air-Water Gas Transfer, Heidelberg, Germany, July 1995.

[13]Venås, B., Sætran, L. R., and Fossdal, J. B., "Wave Induced Wind Fluctuations Relevant to Sea Skimming Missile Flight," AIAA Paper 97-0638, Jan. 1997.

[14]von Kármán, T., "Progress in the Statistical Theory of Turbulence," *Proceedings of the National Academy of Sciences of the United States of America*, Vol. 34, No. 11, National Academy of Sciences, Washington, DC, 1948, pp. 530–539.

[15]*Flying Qualities of Piloted Airplanes*, MIL-F-8785C, 1986.

[16]Hinze, J. O., *Turbulence*, 2nd ed., McGraw–Hill, New York, 1975.

[17]Tielemann, H. W., "A Survey of the Turbulence in the Marine Surface Layer for the Operation of Low-Reynolds Number Aircraft," Virginia Polytechnic Inst. and State Univ., VPI-E-85-10, Blacksburg, VA, March 1985.

[18]Hasselmann, D. E., Dunckel, M., and Ewing, J. A., "Directional Wave Spectra Observed During JONSWAP 1973," *Journal of Physical Oceanography*, Vol. 10, Aug. 1980, pp. 1264–1280.

[19]Bendat, J. S., and Piersol, A. G., *Engineering Applications of Correlation and Spectral Analysis*, Wiley, New York, 1993.

Color reproductions courtesy of Norwegian University of Science and Technology